JOURNAL OF VIROLOGY, July 2007, p. 6785–6797 Vol. 81, No. 13
0022-538X/07/$08.00+0 doi:10.1128/JVI.00198-07

Coxsackievirus B3 Proteins Directionally Complement Each Other To Downregulate Surface Major Histocompatibility Complex Class I[▽]

Christopher T. Cornell,[1]† William B. Kiosses,[2] Stephanie Harkins,[1] and J. Lindsay Whitton[1]*

Molecular and Integrative Neurosciences Department[1] and Core Microscopy Facility,[2] The Scripps Research Institute, La Jolla, California

Received 29 January 2007/Accepted 3 April 2007

Picornaviruses carry a small number of proteins with diverse functions that subvert and exploit the host cell. We have previously shown that three coxsackievirus B3 (CVB3) proteins (2B, 2BC, and 3A) target the Golgi complex and inhibit protein transit. Here we investigate these effects in more detail and evaluate the distribution of major histocompatibility complex (MHC) class I molecules, which are critical mediators of the $CD8^+$ T-cell response. We report that concomitant with viral protein synthesis, MHC class I surface expression is rapidly downregulated during infection. However, this phenomenon may not result solely from inhibition of anterograde trafficking; we propose a new mechanism whereby the CVB3 2B and 2BC proteins upregulate the internalization of MHC class I (and possibly other surface proteins), perhaps by focusing of endocytic vesicles at the Golgi complex. Thus, our findings indicate that CVB3 carries at least three nonstructural proteins that directionally complement one another; 3A disrupts the Golgi complex to inhibit anterograde transport, while 2B and/or 2BC upregulates endocytosis, rapidly removing proteins from the cell surface. Taken together, these effects may render CVB3-infected cells invisible to $CD8^+$ T cells and untouchable by many antiviral effector molecules. This has important implications for immune evasion by CVB3.

Upon infection of a susceptible organism, viruses elicit immunological responses that range from antibody production to cell-mediated defense mechanisms (46). The tug-of-war that results is a battle between the ability of the virus to outpace or circumvent various immune surveillance strategies and its ability to maintain replicative fitness to reach the ultimate goal of transmission to the next suitable host. Alternatively, successful evasion of the immune system can result in viral persistence, which can exist for the entire life span of the host. Viruses with genomes that encode a vast array of protein products (e.g., herpesviruses) employ immune evasion strategies on multiple levels, including the inhibition of major histocompatibility complex (MHC) antigen presentation, the reduction of surface cytokine receptors and costimulatory molecules, and even the production of molecules that resemble immunosuppressive cytokines (e.g., interleukin-10 [IL-10]) (21).

Smaller RNA viruses, including members of the *Picornaviridae* family, carry a very limited number (~12) of protein products and therefore must rely heavily on the multifunctional nature of these polypeptides, not only for their various roles in replication and gene expression but also for their ability to act as mediators of immune evasion within the host (8). It has been known for some time that many of the picornavirus nonstructural proteins, as well as their precursors, directly associate with intracellular membranes (5, 17, 40, 41). This association triggers the rearrangement of these membranes into vesicles that take on a rosette-like appearance and provide a platform on which the viral RNA genome is replicated (18). As with many other viruses that extensively modify the intracellular space, the effects of membrane rearrangement have been shown to dramatically reduce anterograde protein trafficking (7, 11, 14, 15), as subcellular components of the Golgi complex and endoplasmic reticulum (ER) are commandeered for RNA amplification and progeny virus production. Thus far, the general theme of host secretion shutoff holds true for most picornaviruses that have been examined, although the viral proteins that participate in this process are not absolutely conserved (6, 28). It is intriguing to think that picornaviruses have, despite their very small number of gene products, specialized protein functions aimed specifically at immune evasion. However, given the wide array of functions ascribed to each of the polypeptides they express, these viruses have more than likely been subjected to evolutionary pressures within their hosts that have forced them to develop replicative strategies that go hand in hand with circumventing immune detection.

A select group of picornavirus nonstructural proteins have been shown to have antisecretory effects. Early work by Barco and Carrasco showed that for poliovirus, the prototypic picornavirus, 2BC expression was capable of inducing secretion shutoff in *Saccharomyces cerevisiae* (3). Studies from Kirkegaard and coworkers clearly showed that an additional poliovirus protein, 3A, is capable of inhibiting ER-to-Golgi transit, resulting in the shutoff of nascent MHC class I/peptide complex trafficking and the downregulation of antiviral cytokine secretion (9, 13). Interestingly, this same ER-to-Golgi shutoff function has been ascribed to the 2BC protein of foot-and-mouth disease virus, whose 3A polypeptide does not appear to have this activity (28). Furthermore, both our work and results published by de Jong et al. (12) have shown that the coxsackievirus B3 (CVB3) 2B protein is capable of associating with and blocking trafficking through the Golgi complex, an effect

* Corresponding author. Mailing address: Molecular and Integrative Neurosciences Department, The Scripps Research Institute, 10550 N. Torrey Pines Rd., La Jolla, CA 92037. Phone: (858) 784-7090. Fax: (858) 784-7380. E-mail: lwhitton@scripps.edu.

† Present address: Biopharmaceutical Department, Allergan, Inc., 2525 Dupont Dr., Irvine, CA 92612.

▽ Published ahead of print on 18 April 2007.

thought to be mediated by a disruption in calcium homeostasis (11, 42). We have additionally shown that the 2BC precursor displays an enhanced ability to block Golgi complex throughput, also via direct physical targeting of this organelle (7). In addition to the CVB3 2B and 2BC proteins inhibiting protein transit through the Golgi complex, we have also shown that the coxsackievirus 3A protein, the most potent inhibitor of protein secretion, disrupts this organelle completely (7).

Our previously published work clearly demonstrated that three CVB3 proteins (2B, 2BC, and 3A) each target the Golgi complex and inhibit protein secretion to various degrees. In an attempt to extend these observations and place them in the context of CVB3 immune evasion, herein we present data that reveal the effects of these three proteins on the cell surface expression of MHC class I, which is an absolute requirement for $CD8^+$ T-cell recognition of virus-infected cells. Our results confirm that 3A reduces surface MHC class I levels, and we also identify a new feature which may further aid CVB3 in evading host immune responses, namely, the increased internalization of MHC class I (and possibly other proteins) by 2B and 2BC. At ~3 h postinfection, when viral proteins first become readily detectable, MHC class I complexes are internalized from the surface at a higher rate than that of normal cellular turnover, suggesting a virus-induced acceleration of endocytosis. Strikingly, even at late times post-CVB3 infection, anterograde trafficking is severely reduced but not completely halted, suggesting (i) that these previously unknown effects of 2B and/or 2BC may be critical for mediating the internalization of viral peptide complexes/MHCs that escape the profound but incomplete trafficking blockade imposed by 3A and (ii) the existence of an intracellular subcompartment, distinct from the Golgi complex, that is left intact during a CVB3 infection and may act as a focus for endocytic vesicles. These results have implications that may extend beyond MHC class I downregulation in vivo.

MATERIALS AND METHODS

Plasmids and chemicals. The cloning of pCMV-DsRed(mem)-CVB3, from which infectious DsRed(mem)-expressing CVB3 was derived, has been described previously, as have the dicistronic enhanced green fluorescent protein [EGFP-(mem)] reporter constructs used in this study (7). Cycloheximide and guanidine hydrochloride were purchased from Calbiochem (San Diego, CA), and brefeldin A (BrA) was obtained from Sigma (St. Louis, MO).

Cells and viruses. The production of wild-type (from plasmid pH 3, a kind gift from Kirk Knowlton, University of California, San Diego) and DsRed(mem) coxsackieviruses has been described previously (7, 25). All cell culture studies utilized HeLa (RW) cells (procured from Rainer Wessely, UC San Diego) maintained in Dulbecco's modified Eagle's medium (DMEM; Invitrogen, Carlsbad, CA) supplemented with 10% fetal bovine serum, 2 mM L-glutamine, 100 U/ml penicillin, and 100 μg/ml streptomycin. Cells were grown at 37°C in 5% CO_2.

Western blots. Western blotting was carried out by first resolving protein lysates in a 4 to 20% gradient polyacrylamide gel containing sodium dodecyl sulfate (Invitrogen, Carlsbad, CA), electroblotting the proteins onto a Protran nitrocellulose membrane (Schleicher and Schuell Bioscience, Keene, NH), and then blocking the membrane in 5% dry milk in phosphate-buffered saline (PBS). Following a wash step consisting of 0.05% Nonidet P-40 in PBS, an anti-3A rabbit polyclonal antibody (diluted 1:1,000 in blocking solution plus 0.05% NP-40) (7) was incubated with the membrane for 1 hour. Excess primary antibody was washed off the membrane, and a 1:5,000 dilution of a goat anti-rabbit secondary antibody conjugated to horseradish peroxidase (BD Biosciences/Pharmingen, San Diego, CA) was added for 30 minutes. Antibody-target complexes were revealed using SuperSignal West Pico chemiluminescence substrate (Pierce Biotechnology, Rockford, IL), followed by exposure of the membrane to BioMax MR film (Eastman Kodak, Rochester, NY).

Citrate-phosphate wash time course experiments. Citrate-phosphate buffer (pH 3.0) was prepared by adding 10.2 ml of 0.2 M dibasic sodium phosphate to 39.8 ml 0.1 M citric acid and then adding distilled and deionized water to a final volume of 100 ml. Following CVB3 infection (multiplicity of infection [MOI] of 10) or mock treatment for 40 min, HeLa (RW) cell monolayers were harvested in PBS by use of a rubber policeman, centrifuged for 8 min at 1,200 × *g*, and resuspended in citrate-phosphate buffer (1 ml per 10^6 cells) for 1 min. The low pH was rapidly quenched by adding 15 ml of DMEM. The cells were centrifuged for 8 min at 1,200 × *g*, washed once in 5 ml DMEM, and pelleted again. Cell pellets were resuspended in DMEM at a concentration of 5×10^6 cells/ml, transferred to sterile snap-cap tubes, and placed in a 37°C incubator containing 5% CO_2, with or without the addition of inhibitor (cycloheximide at 100 μg/ml or guanidine hydrochloride at 2 mM). At various times postwash, 0.2 ml cell suspension was removed and transferred to a 96-well round-bottomed plate, centrifuged for 3 min at 1,200 × *g*, washed twice in PBS, and stained with mouse anti-human β_2-microglobulin (anti-β_2M) antibody (conjugated to phycoerythrin; BD Biosciences) for 30 min on ice. The cells were washed twice in PBS and fixed in 2% neutral buffered formalin for flow cytometry analysis. Identical manipulations were carried out for time course experiments that did not involve a citrate-phosphate washing step.

Flow cytometry. Cells were analyzed on a FACSCalibur flow cytometer (BD Biosciences, San Jose, CA) running BD CellQuest software, and the resulting data were analyzed using FloJo software, version 6.1 (Tree Star, Ashland, OR).

Immunofluorescence reagents and immunocytochemistry. 4′,6-Diamidino-2-phenylindole (DAPI) was obtained from Invitrogen/Molecular Probes (Eugene, OR) and used at a final concentration of 0.3 μM. Mouse anti-HLA-ABC (clone W6/32) and rabbit anti-giantin were procured from Abcam (Cambridge, MA), and mouse anti-human β_2M (conjugated to R-phycoerythrin) was obtained from BD Pharmingen (San Diego, CA). These antibodies were diluted 1:100 and 1:10, respectively. Goat anti-mouse–tetramethylrhodamine and goat anti-mouse–Alexa 488 (both from Invitrogen/Molecular Probes, Eugene, OR) were diluted 1:250. All immunocytochemistry was carried out as described previously (7), using 2% electron microscopy (EM)-grade, methanol-free paraformaldehyde (Polysciences Inc., Warrington, PA). When necessary, cell permeabilization was achieved by incubating cells in the presence of 0.1% Triton X-100 in PBS for 5 minutes. For all confocal microscopy studies, cells were grown on cover glass, stained, mounted onto slides by using VectaShield mounting medium (Vector Labs, Burlingame, CA), and sealed with clear nail polish.

Confocal microscopy and image analysis. Samples were visualized on a Rainbow Radiance 2100 laser scanning confocal system attached to a Nikon TE2000-U inverted microscope (Bio-Rad–Zeiss). Laser Sharp 2000 software was used to acquire *z*-series images, which were analyzed with Image J (NIH Imaging [http://rsb.info.nih.gov/ij]) and Image Pro Plus 3DS (Media Cybernetics, Silver Spring, MD) to determine the mean fluorescence intensity (MFI) of surface and/or intracellular MHC class I. A ratiometric analysis was done by comparing the fluorescence of EGFP(mem)-positive cells to that of untransfected/mock-transfected cells. The Image J program was also used to generate the *z*-profile sections analyzed in this study.

AM4-65 dye studies. To track endosomes, AM4-65 dye (Biotium, Hayward, CA) was added to live HeLa cell monolayers at 16 h posttransfection, at a final concentration of 1 μM in complete DMEM containing 10% fetal bovine serum. Following a 10-second incubation at room temperature, the dye-medium mix was removed, and the cells were fixed immediately in 2% EM-grade paraformaldehyde (Polysciences Inc., Warrington, PA) in PBS for 5 min. Cover glasses were mounted as described above.

RESULTS

CVB3 infection causes a reduction in surface MHC class I heterodimers. Viral epitopes are presented to $CD8^+$ T cells by cell surface MHC class I heterodimers comprising the membrane-anchored class I heavy chain, together with β_2M. To determine the kinetics with which CVB3 infection could impact the overall level of surface MHC class I heterodimers, we infected HeLa (RW) cells with wild-type CVB3 at an MOI of 10. Beginning immediately after the adsorption step ($t = 0$), a 7-hour time course experiment was carried out, during which we harvested, at each hour, equal numbers of infected and

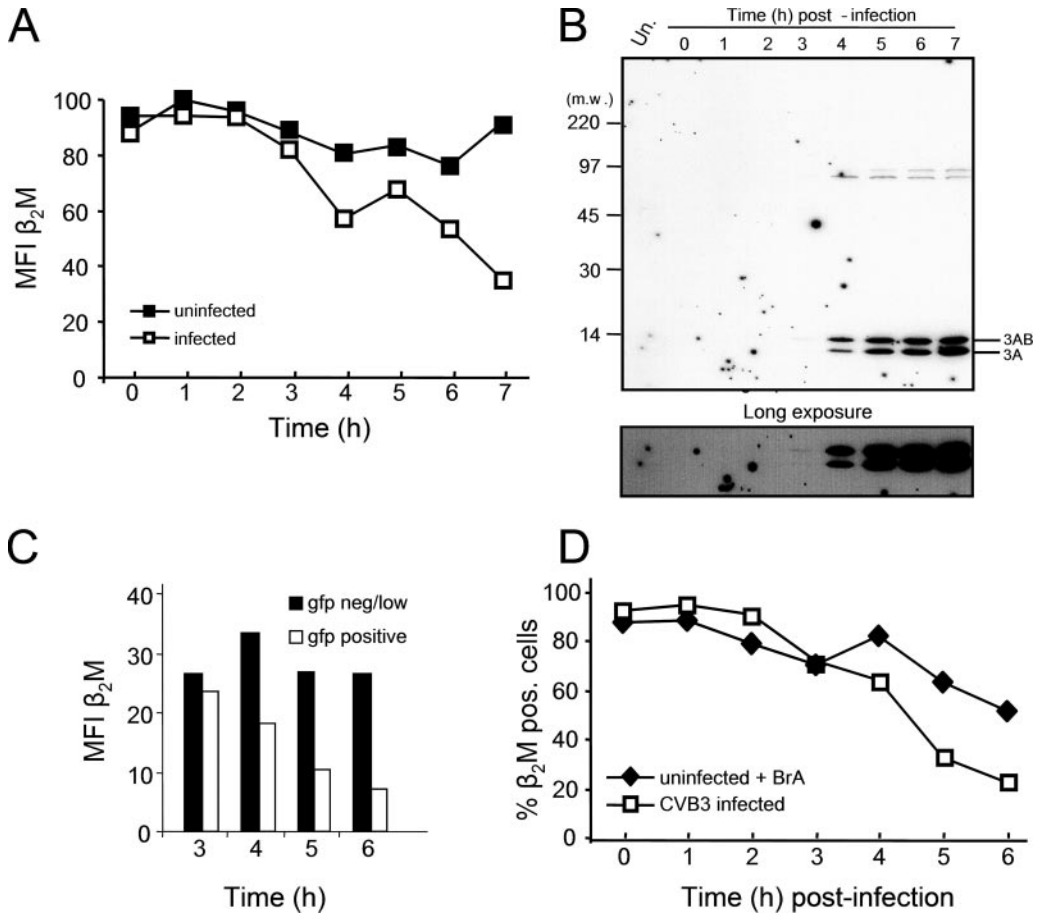

FIG. 1. CVB3 gene expression correlates with the downregulation of surface MHC class I. All experiments were repeated at least three times, and results are shown for a single representative experiment. (A) HeLa (RW) cells were mock infected or infected with wild-type CVB3 at an MOI of 10. Following virus adsorption, cells were harvested, washed, and incubated in suspension at 37°C with 5% CO_2. At the indicated times postharvest, an aliquot of cells from each culture was stained with mouse anti-human β_2M antibody, fixed, and analyzed by flow cytometry to assess surface MHC class I levels (MFI β_2M). (B) During the experiment depicted in panel A, cell lysates from the CVB3 infection time course were subjected to sodium dodecyl sulfate-polyacrylamide gel electrophoresis and Western blot analysis to examine the onset of viral protein expression. A rabbit anti-3A antibody detected the mature 3A protein as well as the immediate precursor polypeptide 3AB (indicated to the right of the panel). A longer exposure of this region of the blot is shown below. (C) Comparison of uninfected and infected cell surface MHC class I expression within a single-cell population. HeLa (RW) cells were infected at a low MOI (0.1) with a recombinant CVB3 that expresses EGFP, and surface staining (as in panel A) was carried out to assess MHC class I levels on the surfaces of uninfected (black bars) versus infected (white bars) cells, which were distinguished based on the expression of GFP, which became detectable at ~3 h postinfection. (D) HeLa (RW) cells were mock infected or infected with CVB3 at an MOI of 10. Following virus adsorption, both cell populations were harvested, washed, and incubated in suspension at 37°C with 5% CO_2. Two μg/mL brefeldin A (BrA) was added to the uninfected population immediately postharvest, and at the indicated times, an aliquot of cells from each population was stained with mouse anti-human β_2M antibody. The cells were then fixed and analyzed by flow cytometry to assess the percentage of cells that were positive for β_2M expression.

uninfected cells, stained them using a fluorochrome-labeled antibody specific for β_2M, and measured the staining intensities on individual cells by flow cytometry. A comparison between the MFIs of the uninfected (black squares) and infected (white squares) cell populations (Fig. 1A) revealed that while MHC class I levels remained approximately equal for the first 3 hours of the time course, a noticeable reduction in the level of this molecule occurred in the infected cell population around 4 hours postinfection. At the end of the time course ($t = 7$), the level of MHC class I expressed at the surface on the infected cell population was less than half that for uninfected cells.

In a parallel time course, depicted in Fig. 1B, we analyzed CVB3 viral protein synthesis levels, using the appearance of the 3AB precursor and mature 3A viral polypeptides on a Western blot as a marker for viral translation. Figure 1B shows a Western blot probed with a rabbit polyclonal antiserum directed against a peptide from the amino terminus of 3A, a reagent previously developed by our laboratory (7). As shown in the upper panel, these viral proteins were readily detected at 4 hours postinfection, and a longer exposure (lower panel) showed that the proteins were present at 3 h postinfection. This corresponds closely with the reduction in surface MHC class I (Fig. 1A), thereby temporally linking viral gene expression to cell surface MHC downregulation.

We considered it likely that the downregulation of MHC class I shown in Fig. 1A was the result of individual cells' infection status, but it was possible that the phenomenon might

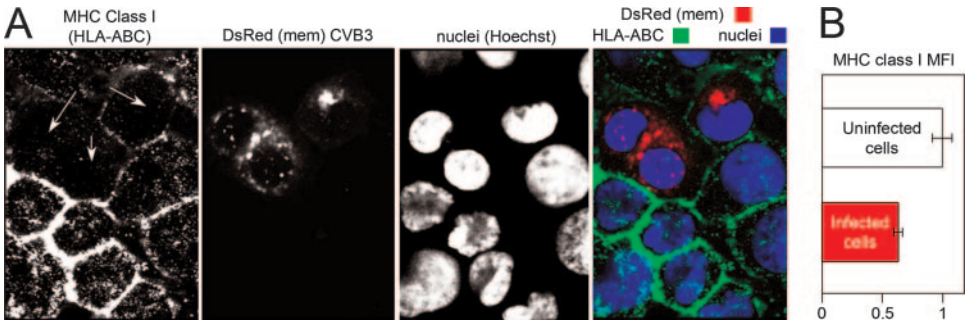

FIG. 2. Confocal microscopy confirms reduced levels of MHC class I on the surfaces of CVB3-infected cells. (A) A recombinant CVB3 carrying a membrane-targeted version of DsRed protein has been described previously by our laboratory (7). HeLa (RW) cells grown in monolayers on cover glass were infected with DsRed(mem) CVB3 at a low MOI (0.1) and fixed at 5 h postinfection. A monoclonal antibody recognizing a common HLA heavy chain epitope (HLA-ABC; clone W6/32) was used to stain unpermeabilized cells for MHC class I analysis by confocal microscopy. *z*-series images (encompassing the entire plasma membrane region) were acquired and projected using ImageJ, and the mean fluorescence was measured. Grayscale images of MHC class I (stained with fluorescein isothiocyanate), DsRed(mem) protein localization, and DAPI-stained nuclei (blue) are shown (first three panels), along with a merged image (far right panel). The white arrows (left panel) highlight reduced MHC class I on the surfaces of three infected cells that are positive for DsRed(mem) protein expression. (B) Images from 30 to 50 uninfected or infected cells were acquired as described for panel A, and the MFIs of MHC class I staining (with standard errors of the means) were calculated for uninfected and infected cells. The mean MFI for uninfected cells (white bar) was assigned the value 1.0, and the MFI for infected cells (red bar) is shown relative to that value.

be an effect exerted in *trans*, perhaps from cellular responses to molecules secreted as a result of infection. To distinguish between these two possibilities, we next infected cells at a low MOI and compared surface levels of MHC class I on uninfected and infected cells within the same cell population. HeLa (RW) cells were infected (at an MOI of 0.1) with a previously described recombinant CVB3 that expresses EGFP (EGFP-CVB3) (20), and flow cytometry was used to evaluate surface MHC class I expression on EGFP-negative/low cells (uninfected) and on EGFP-positive (infected) cells. GFP expression—like that of native virus proteins (Fig. 1B)—was first detected at approximately 3 h postinfection, and thus the values from this time point forward were graphed in Fig. 1C. While the level of surface MHC class I on uninfected cells remained relatively stable throughout the time course (black bars), EGFP-positive (i.e., infected) cells displayed rapidly declining levels of surface MHC class I (white bars). Consistent with our end-point observation in Fig. 1A, the level of surface MHC class I in the infected cells was less than half that observed for the uninfected cell population.

To begin to assess the mechanism by which CVB3 downregulates levels of surface MHC class I, we sought to determine if virus infection alters the rate of MHC class I internalization. We carried out a similar time course to that shown in Fig. 1A, this time comparing CVB3-infected HeLa cells to a separate population of cells that had been treated with the fungal metabolite BrA. BrA quickly dissociates the Golgi complex by inhibiting ADP ribosylation factor-dependent vesicle formation, thereby completely blocking anterograde secretory transport (16); therefore, the rate of decrease in surface MHC class I levels in BrA-treated cells provides a readout of the rapidity with which the cell normally internalizes surface MHC. Figure 1D shows that for the first 3 hours of the time course, levels of MHC class I on infected (squares) and BrA-treated (diamonds) cells were roughly equal. However, between 4 and 6 h posttreatment, there was a more rapid reduction in surface MHC class I on CVB3-infected cells than on BrA-treated cells, indicating that the loss of MHC from the surfaces of infected cells was not simply due to the shutoff of anterograde trafficking of new molecules. These observations led us to propose that in addition to restricting anterograde trafficking via disrupting the Golgi complex, CVB3 infection further limits the expression of virus-specific MHC-peptide complexes by increasing the rate of MHC internalization.

Confocal microscopy confirms CVB3-mediated MHC class I downregulation. We previously generated a recombinant CVB3 that expresses DsRed(mem), a form of red fluorescent protein targeted to the plasma membrane, and examined the distribution of this marker protein to ascertain the effects of virus infection on protein trafficking and distribution, using laser scanning confocal microscopy (7). By using this virus rather than a recombinant that expresses a non-membrane-targeted marker (EGFP) (Fig. 1C), one can analyze the subcellular localization of trafficking protein during an infection. In addition to corroborating our flow cytometry results, confocal microscopy provided insight into the possible mechanism(s) responsible for MHC class I downregulation. Figure 2A shows representative images of tissue culture cells infected at a low MOI (0.1) with CVB3-DsRed(mem) virus. At 5 h postinfection, the cells were stained using an HLA-ABC-specific mouse monoclonal antibody, allowing us to directly compare levels of MHC class I on infected (DsRed-positive) and uninfected cells. Three virus-infected cells (indicated by white arrows in the first image and depicted alone in the second panel) are shown, and all of them had lower levels of MHC class I on their surfaces than the adjacent uninfected (DsRed-negative) cells. The last column represents a merged image showing HLA-ABC (green), DsRed(mem) (red), and nuclei stained with DAPI (blue). To measure the CVB3-mediated reduction of MHC class I, a minimum of 50 uninfected and infected cells from at least two independent experiments were assessed for HLA-ABC staining intensity. *z*-series confocal microscopy images from uninfected (white bar) versus infected (red bar) cells were compared (Fig. 2B), and the staining

intensity observed in uninfected cells was normalized to a value of 1. At 5 h postinfection, infected cells displayed an approximately 35% reduction in surface MHC class I, confirming the virus-mediated reduction of surface MHC class I that had been observed by flow cytometry. A 75% reduction was observed for cells analyzed by flow cytometry that had been infected with the EGFP-expressing virus (Fig. 1C); this quantitative difference could be a result of physiological differences in HeLa cells infected in suspension (for flow cytometry experiments) versus monolayers (confocal microscopy studies).

CVB3-mediated MHC downregulation requires RNA replication and is not mediated by host translation shutoff. Picornaviruses have been shown to inhibit anterograde protein trafficking, which could prevent the secretion of antiviral cytokines, the presentation of MHC/viral peptide complexes, or the expression of surface cytokine receptors through which immune effector molecules (e.g., interferons and tumor necrosis factor) exert their antiviral effects (9, 13, 30, 34). To test the effects of CVB3 infection on the kinetics of anterograde protein trafficking, we developed an assay based on a previously published technique (34, 37) whereby surface MHC class I heterodimers are rendered undetectable by a low-pH citrate-phosphate washing step which removes β_2M (Fig. 3A, FL-2 signal representing β_2M on the surfaces of pre- versus post-wash cells). After the acid wash, mock-infected cells and cells infected with CVB3 at a high MOI (~10) were monitored during a time course experiment for the appearance of new MHC class I heterodimers. Immediately postwash ($t = 0$), virtually no cells in any of the populations tested were β_2M positive (Fig. 3B). For the duration of the time course, uninfected cells that had been treated with BrA, which disrupts the Golgi apparatus, displayed very low levels of MHC class I recovery (Fig. 3B, squares). At early time points postwash (between 0 and 3 h), infected cells recovered levels of MHC class I comparable to those observed in uninfected cells (~80% positive cells) (Fig. 3B, compare X's to diamonds), which would be predicted given the low levels of viral protein expressed prior to 3 h postinfection (Fig. 1B). While the uninfected cell population appeared to maintain the same level of MHC class I during the rest of the time course, the CVB3-infected cells rapidly lost their surface MHC class I. We cannot determine from these data whether this reduction resulted from decreased anterograde trafficking, increased internalization, or both; experiments to clarify the mechanisms are reported below. This reduction of surface MHC heterodimers was not observed in infected cells which had been treated with 2 mM guanidine hydrochloride, a known inhibitor of picornavirus RNA synthesis (Fig. 3B, asterisks) (19), which demonstrates that viral RNA replication is required to mediate the reduction in surface MHC class I. Furthermore, to ascertain whether the downregulation of MHC class I from the surfaces of infected HeLa cells was due to the shutoff of host protein synthesis (known to occur during picornavirus infection) (26), we used a cycloheximide-treated, uninfected cell control. In our hands, CVB3-mediated shutoff of host cap-dependent translation occurs at approximately 3 h postinfection (data not shown). The addition of cycloheximide (final concentration, 100 μg/ml) to uninfected cells at 3 h post-citrate wash (Fig. 3B, triangles) revealed that the shutoff of host translation does not result in the MHC class I effect observed during virus infection;

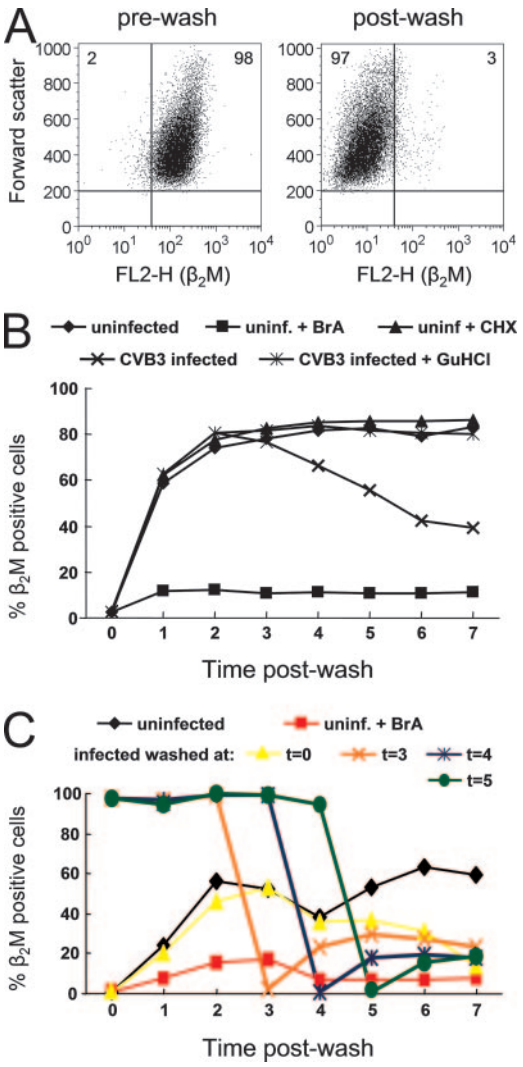

FIG. 3. CVB3 allows trafficking of nascent MHC class I molecules early in infection and then mediates their rapid disappearance. All experiments were repeated at least three times, and the results shown are for a single representative experiment. (A) To ascertain the kinetics of nascent MHC class I trafficking to the cell surface, a citrate-phosphate low-pH wash strategy was employed (34, 37). Before the wash (left panel), flow cytometric analysis indicated that approximately 98% of the cell population stained positive for β_2M (upper right quadrant). Following a citrate-phosphate wash (pH 3.0) for 1 min, preexisting β_2M associated with the MHC class I heavy chain was rendered virtually undetectable within the cell population (right panel, upper left quadrant). (B) HeLa (RW) cells were mock infected or infected with CVB3 at an MOI of 10. Following adsorption, cells were washed with citrate-phosphate buffer as described above. At the indicated time points, the percentage of cells expressing nascent β_2M at the cell surface was measured by flow cytometry and plotted. One sample contained 2 mM guanidine hydrochloride, a known inhibitor of picornavirus RNA synthesis. Two additional uninfected cell populations contained either 2 μg/ml BrA (to halt anterograde secretory transport) or 100 μg/ml cycloheximide (to stop protein synthesis). (C) To analyze anterograde trafficking kinetics at later times postinfection, three acid-washed cell populations were treated exactly as described for panel B (uninfected [black diamonds], infected with CVB3 [yellow triangles], or left uninfected and treated with BrA [red squares]). Three additional populations were CVB3 infected at time zero and washed at 3, 4, or 5 h postinfection (orange, blue, and green plots, respectively).

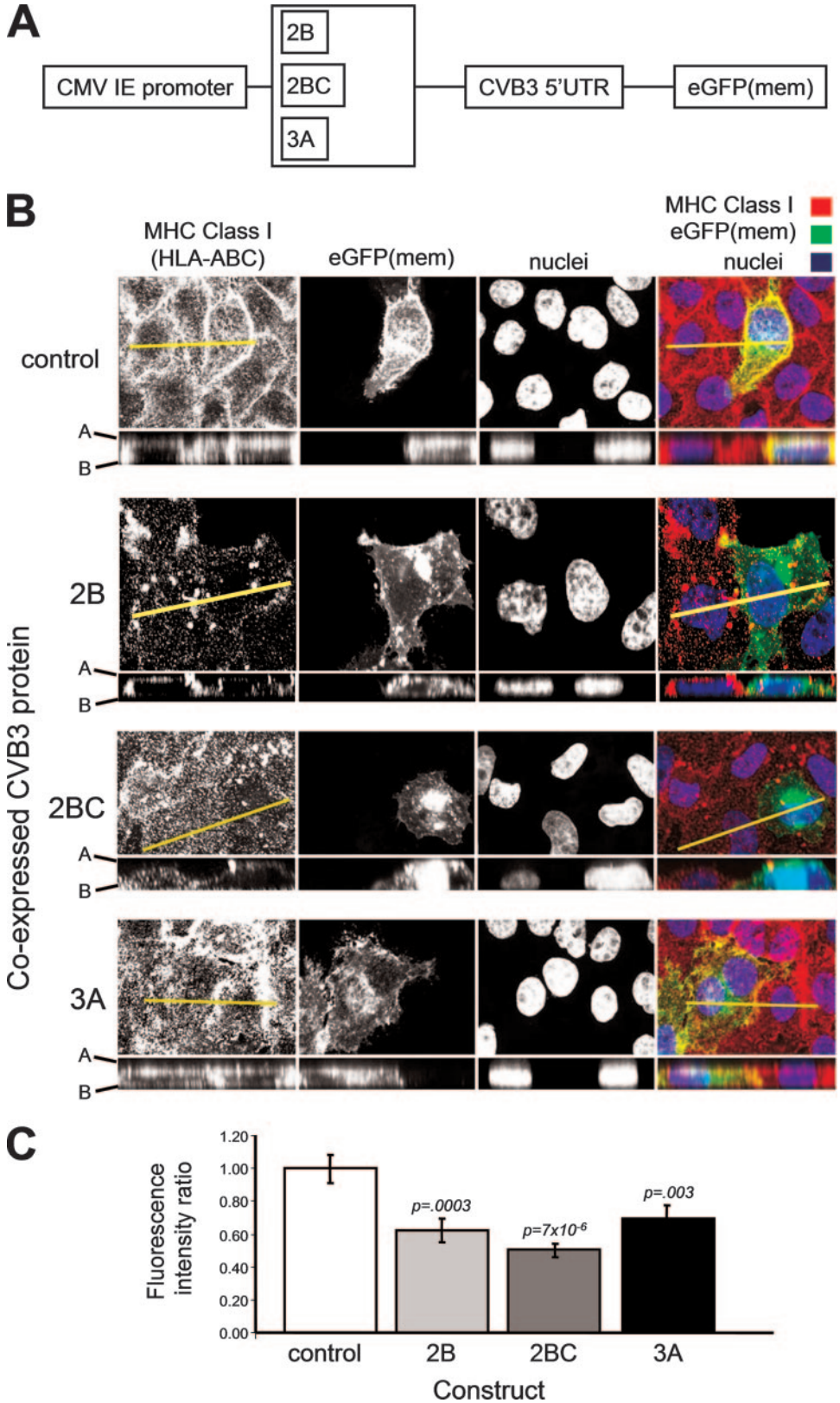

FIG. 4. CVB3 2B, 2BC, and 3A affect MHC class I surface expression to different degrees. (A) Dicistronic reporter plasmids (7) expressed the CVB3 2B, 2BC, or 3A protein together with a membrane-targeted version of EGFP [EGFP(mem)], whose translation was driven by the internal ribosome entry site contained within the CVB3 5′-untranslated region (5′UTR). The control construct (not shown) was the empty parental plasmid, expressing internal ribosome entry site-driven EGFP(mem) but lacking an upstream viral protein. (B) EGFP(mem) expressing dicistronic constructs was transfected into HeLa (RW) cell monolayers, and at 16 h posttransfection, MHC class I (HLA-ABC) (red fluorescence, first

despite cycloheximide treatment, levels of surface MHC class I heterodimers were comparable to those observed in untreated cells.

CVB3 cannot completely prevent anterograde MHC class I trafficking. The data in Fig. 3B show that CVB3-mediated downregulation of surface MHC class I occurs at around 3 h postinfection, corresponding roughly with the onset of viral protein production (Fig. 1B). We predicted that the shutoff of anterograde trafficking mediated by disruption of the Golgi complex (7) was at least partially responsible for the reduction of MHC class I that begins at 3 h postinfection (Fig. 3B). To gain a better understanding of anterograde trafficking function, we applied the citrate-phosphate wash to cells at various times postinfection. Figure 3C shows the results of an experiment that included the three treatments previously described for Fig. 3B (uninfected cells [black diamonds], infected cells [yellow triangles], and BrA-treated cells [red squares]), after each of which cells were washed at the zero time point. Three additional populations were acid washed, at 3, 4, and 5 h postinfection (Fig. 3C, orange, blue, and green plots, respectively), and the kinetics of MHC class I recovery were measured. Surprisingly, despite the successful removal of the MHC class I molecules at three times postinfection, when one would predict a complete shutoff of anterograde trafficking by CVB3, some MHC class I was still able to return to the surface; surface β_2M increased, albeit modestly, immediately postwash in all three populations. Thus, anterograde shutoff during CVB3 infection is profound but incomplete, indicating that some other mechanism is likely to contribute to immune evasion.

Three CVB3 proteins downregulate surface MHC class I to various degrees. We previously utilized dicistronic reporter constructs which express one of three different CVB3 proteins (2B, 2BC, or 3A) together with an EGFP reporter targeted to the plasma membrane [eGFP(mem)] to gain mechanistic insights into how CVB3 disrupts intracellular protein trafficking (Fig. 4A) (7). Our previous results showed that 2B, 2BC, and 3A each inhibit protein trafficking to different degrees. CVB3 3A destroys the Golgi organelle completely to provide a very effective (yet incomplete) blockade to anterograde trafficking, while 2BC and 2B only partially block trafficking by inhibiting protein transit through the Golgi complex. Based on these results, we predicted that when expressed in isolation from its normal viral companions, 3A would be the most effective at reducing surface MHC class I, followed by 2BC and 2B. Figure 4B shows projected *z*-series images of cells transfected separately with the 2B-, 2BC-, and 3A-encoding dicistronic constructs, along with a control construct which expresses EGFP-(mem) in the absence of any CVB3 polypeptides (labeled "control"). Unpermeabilized cells were then stained with HLA-ABC antibody (first column and also represented as red fluorescence in merged images in last column) to reveal surface MHC class I and with DAPI to reveal nuclei (third column and shown in blue in merged images). To facilitate visualization, a profile cut of each *z* series is depicted below each separate grayscale image as well as below each merged image (A, apical; and B, basal). The plane of this profile cut is indicated by the yellow line (first and last columns). The profile images of HLA-ABC staining indicated that MHC staining localized specifically to the cell surface, as intracellular MHC was not readily detected (Fig. 4B, first column). We examined 50 to 100 cells for each of the four different transfections (across a minimum of three experiments) and quantitated surface MHC class I levels by using ImageJ and Image Pro Plus 3DS. Levels of surface MHC class I were compared in transfected versus untransfected cells, and the calculated ratio for control transfected cells (those expressing the GFP marker but no CVB3 proteins) was set to 1. This value, along with the relative ratios for the 2B-, 2BC-, and 3A-expressing cell populations, is shown in Fig. 4C. Cells expressing the 2B protein displayed a level of MHC class I that was reduced approximately 40% compared to that for control transfected cells (represented by a drop in ratio from 1.0 to 0.62 in the presence of 2B). This was surprising, since our previous studies indicated that 2B possesses only a limited degree of antisecretory activity, as measured by a chemiluminescence-based secreted alkaline phosphatase (SEAP) assay (7). Figure 4C also reveals that 2BC displays an enhanced ability over 2B in reducing levels of surface HLA-ABC, resulting in a ratiometric value of 0.5 (a 50% reduction compared to control cells), which presumably reflects the previously reported increased antisecretory activity of this protein. Strikingly, the 3A protein expressed in isolation was the least effective at reducing surface MHC class I, lowering the measured intensity ratio for these cells to 0.7 (an ~30% reduction compared to the control population). Given that 100% of cells expressing the 3A construct have no discernible Golgi apparatus, (7), these data suggest that, as proposed previously (Fig. 1D), the greater reductions caused by the 2B and 2BC proteins may reflect increased rates of endocytosis in these transfected cells and that this effect, which is absent in the 3A transfectants, contributes markedly to the reduction observed in infected cells (Fig. 1D). This observation could not have been made using our previously published SEAP assay system, in which the trafficking protein is secreted rather than membrane-bound, thereby allowing the SEAP marker to escape the internalization activities of 2B and/or 2BC. We propose that during CVB3 infection, a combination of viral polypeptides that includes 2B, 2BC, and 3A "directionally complement" one another to rapidly downregulate MHC class I.

To confirm the fluorescence intensity measurements shown in Fig. 4C, we carried out the same transfection analysis and

column) and nuclei (blue fluorescence, third column) were stained. Cells were left unpermeabilized so that only surface MHC class I was revealed. Confocal *z*-series images were acquired, and *z*-dimensional profiles, shown below each image, were generated along the *x*-*y* axes indicated by the yellow lines (first column). A and B, apical and basal sides of the cell monolayers, respectively. Merged images for each of the four constructs tested are shown in the last column. (C) A series of cells from a minimum of three independent transfection experiments (as depicted in panel A) were analyzed for surface MHC class I expression relative to that of a mock-transfected control. The values shown represent normalization to the control construct. Student's *t* test (*P* values are given above bars) was done, comparing 2B, 2BC, or 3A to the control.

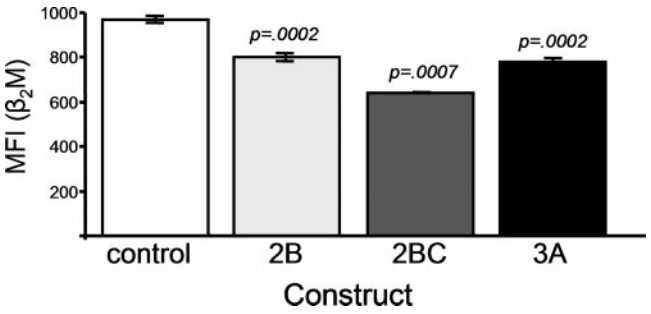

FIG. 5. Differing effects of three CVB3 proteins on levels of surface MHC class I heterodimers, as confirmed by flow cytometry. Cells were transfected with EGFP(mem)-expressing dicistronic constructs (depicted in Fig. 4A) that coexpressed CVB3 2B, 2BC, or 3A or no viral protein (control construct). At 16 h posttransfection, cells were harvested, and their surface β_2M levels were measured by staining with an anti-β_2M antibody conjugated to phycoerythrin. The MFI of the β_2M signal present on the surfaces of GFP-positive cells was measured and graphed. Student's *t* test was done to compare the control to each of the three constructs, and the *P* values are depicted above the bars.

utilized a flow cytometer to analyze MHC class I levels on the surfaces of tens of thousands of transfected cells by measuring β_2M MFIs (Fig. 5). While the overall reduction of MHC class I heterodimers was less pronounced, the relative activities of the three CVB3 proteins were the same as those depicted in Fig. 4C, and the differences were statistically highly significant.

CVB3 2B and 2BC induce a clustering of MHC class I around the Golgi complex. We next wanted to examine the intracellular locations of MHC class I molecules in the presence and absence of CVB3 protein expression to gain a better understanding of the mechanism by which 3A, 2B, and 2BC mediate downregulation of these molecules. To this end, we carried out the same experiment as that depicted in Fig. 4B, but this time we permeabilized the cell monolayers with detergent to facilitate the staining of intracellular MHC molecules in addition to those residing on the cell surface (Fig. 6A). In the absence of CVB3 protein expression (top row), HLA-ABC staining (first column) revealed an even distribution of MHC class I on the surface and in vesicular structures inside the cell. This was true for transfected [EGFP(mem)-positive] cells (Fig. 6A, second column) as well as untransfected surrounding cells. The profile view of MHC class I staining (small panel below far left image) showed a faint perinuclear staining pattern that likely represents MHC class I trafficking through the Golgi subcompartment. Strikingly, in cells expressing 2B (second row) or 2BC (third row), the proportion of MHC found within this subcompartment dramatically increased. To confirm this observation, we used an antibody directed at giantin, a major component of the Golgi complex, along with the HLA-ABC antibody to costain this organelle in 2BC-transfected cells (Fig. 6B). HLA-ABC (first image) showed distinct colocalization with the giantin marker (fourth image and merged image at far right), indicating that MHC class I resides largely in the Golgi subcompartment in the presence of 2BC. We propose that the pulldown of MHC class I initially observed during infection and subsequently shown to be mediated by 2B and/or 2BC is a result of the retrograde translocation of MHC from the plasma membrane to the Golgi subcompartment.

We also analyzed the subcellular localization of MHC class I molecules in the presence of CVB3 3A expression (Fig. 6A, bottom row). The HLA-ABC signal was found not only on the cell surface but also scattered throughout the cytoplasm (first image and *z* profile just below). Since virtually 100% of cells expressing CVB3 3A at this time point have a completely disrupted Golgi organelle (7), the modest levels of MHC class I internalized in the presence of 3A (Fig. 4) likely have no subcompartment destination within the transfected cell and therefore take on the randomly dispersed pattern observed in Fig. 6A.

2B and 2BC increase targeting of endocytic vesicles to the Golgi complex. Finally, we wished to directly test our hypothesis that 2B and 2BC mediate the internalization of surface MHC class I by upregulating the rate of endocytosis. AM4-65 is a lipophilic styryl dye that exhibits bright red fluorescence when associated with membranes but remains nonfluorescent in its unbound state (4). Due to its lipophilic nature, its entry into the cell depends on endocytosis; therefore, it can be used not only to measure the overall rate of endocytosis but also to reveal the intracellular location of recently internalized endosomes. We transfected cells with the EGFP(mem) constructs, and at 16 h posttransfection, we subjected the live cells to a 10-second treatment with AM4-65 dye before fixation (Fig. 7A). For control cells, AM4-65-labeled endosomes can be seen scattered throughout the cytoplasm (top row, first image) of transfected and untransfected cells (which can be distinguished by GFP expression) (Fig. 7A, columns three and four). Interestingly, in the presence of 2B (second row) or 2BC (third row), endosomes appear to focus in and around the Golgi complex (white arrows; compare GFP-positive with GFP-negative cells). This is particularly apparent in the images depicted for 2BC-transfected cells, which show a perinuclear overlap between EGFP(mem) and the AM4-65 signal (green and red fluorescence in the merged image). In the presence of the 3A protein, AM4-65 fluorescence is scattered in a vesicular pattern throughout the cell (bottom row). Cells expressing 3A lack a Golgi complex, and therefore newly endocytosed vesicles are without a major subcompartment destination, which is likely the reason for this observed pattern.

To produce quantitative results related to our analysis of AM4-65 distributions in the presence and absence of CVB3 protein expression, we calculated the areas of transfected cells positive for AM4-65 fluorescence and evaluated the statistical significance of any differences (Fig. 7B). In control cells which expressed no CVB3 protein, approximately 55% of the cell area was occupied by newly endocytosed vesicles (white bar). In striking contrast, this value was much smaller for both 2B- and 2BC-expressing cells, which displayed approximately 20% of the cell area as positive for AM4-65 (light gray and dark gray bars, respectively), confirming the focusing effect observed in Fig. 7A. 3A-expressing cells (black bar) showed a distribution of fluorescence that closely mimicked that observed in control cells, indicating an absence of this focusing effect.

DISCUSSION

Our previous work showed that three CVB3 proteins (2B, 2BC, and 3A) are each capable of targeting the host secretory apparatus to mediate protein trafficking shutoff (7). The present study addresses the effects that these proteins have on

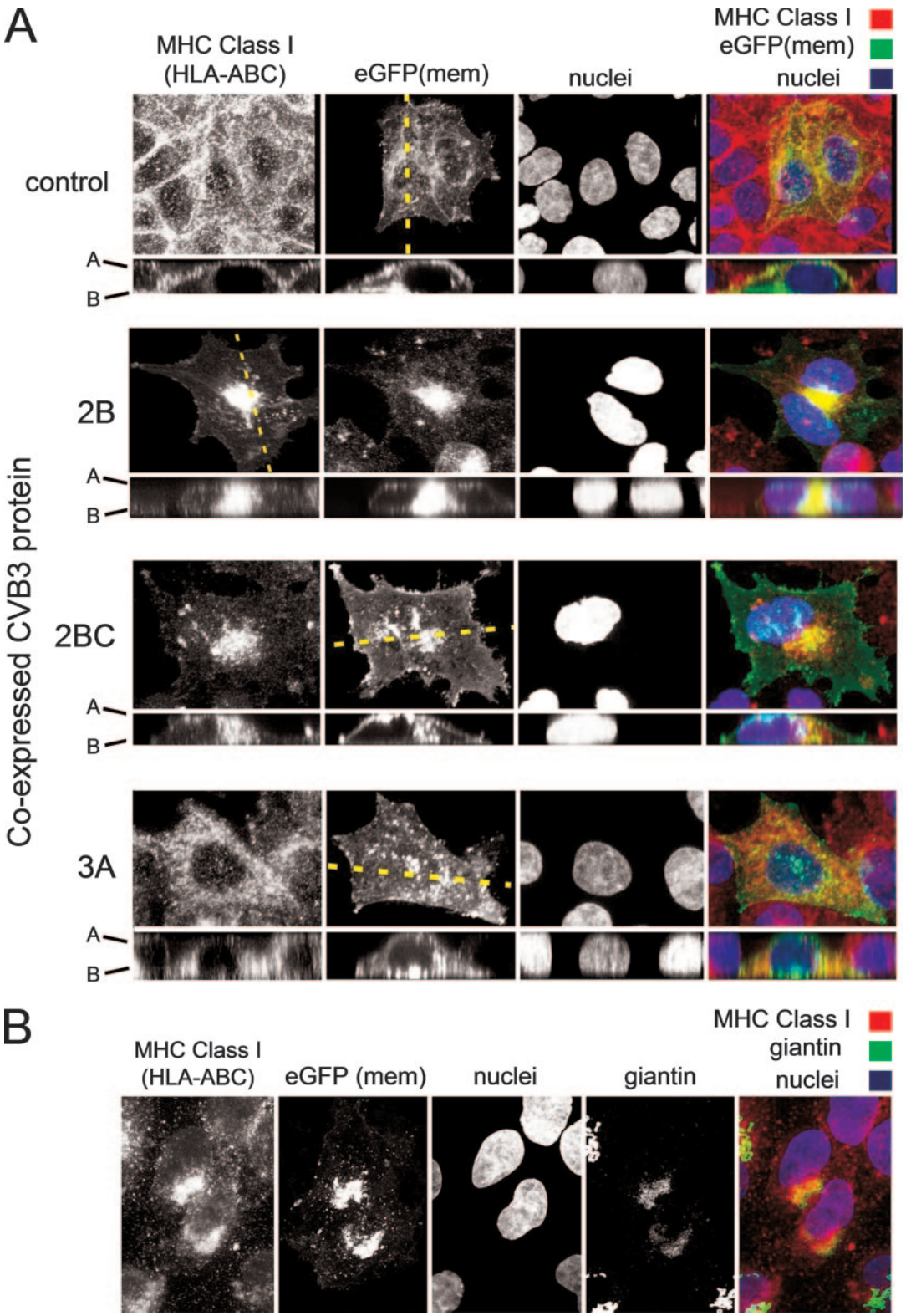

FIG. 6. MHC class I is redistributed to the Golgi region in the presence of CVB3 2BC. (A) EGFP(mem)-expressing dicistronic constructs were transfected into HeLa (RW) cell monolayers, and at 16 h posttransfection, MHC class I (HLA-ABC) (red fluorescence, first column) and nuclei (blue fluorescence, third column) were stained. In contrast to the approach taken in Fig. 4, the cells depicted here were subjected to a permeabilization step prior to HLA-ABC staining to reveal not only surface but also intracellular MHC class I localization. Confocal *z*-series images were acquired, and *z*-dimensional profiles, shown below each image, were generated along the *x*-*y* axes indicated by the yellow lines. A and B, the apical and basal sides of the cell monolayers, respectively. Merged images for each of the four constructs tested are shown in the last column. (B) To assess the localization of intracellular MHC class I relative to the Golgi complex in cells expressing 2BC, cells transfected with this construct were stained using a rabbit polyclonal antibody to giantin, a major component of the Golgi complex (fourth column; depicted as green fluorescence in the merged image). HLA-ABC staining is depicted in red as described above, and nuclei were revealed by staining with DAPI. The merged image shows colocalization between MHC class I and the Golgi subcompartment.

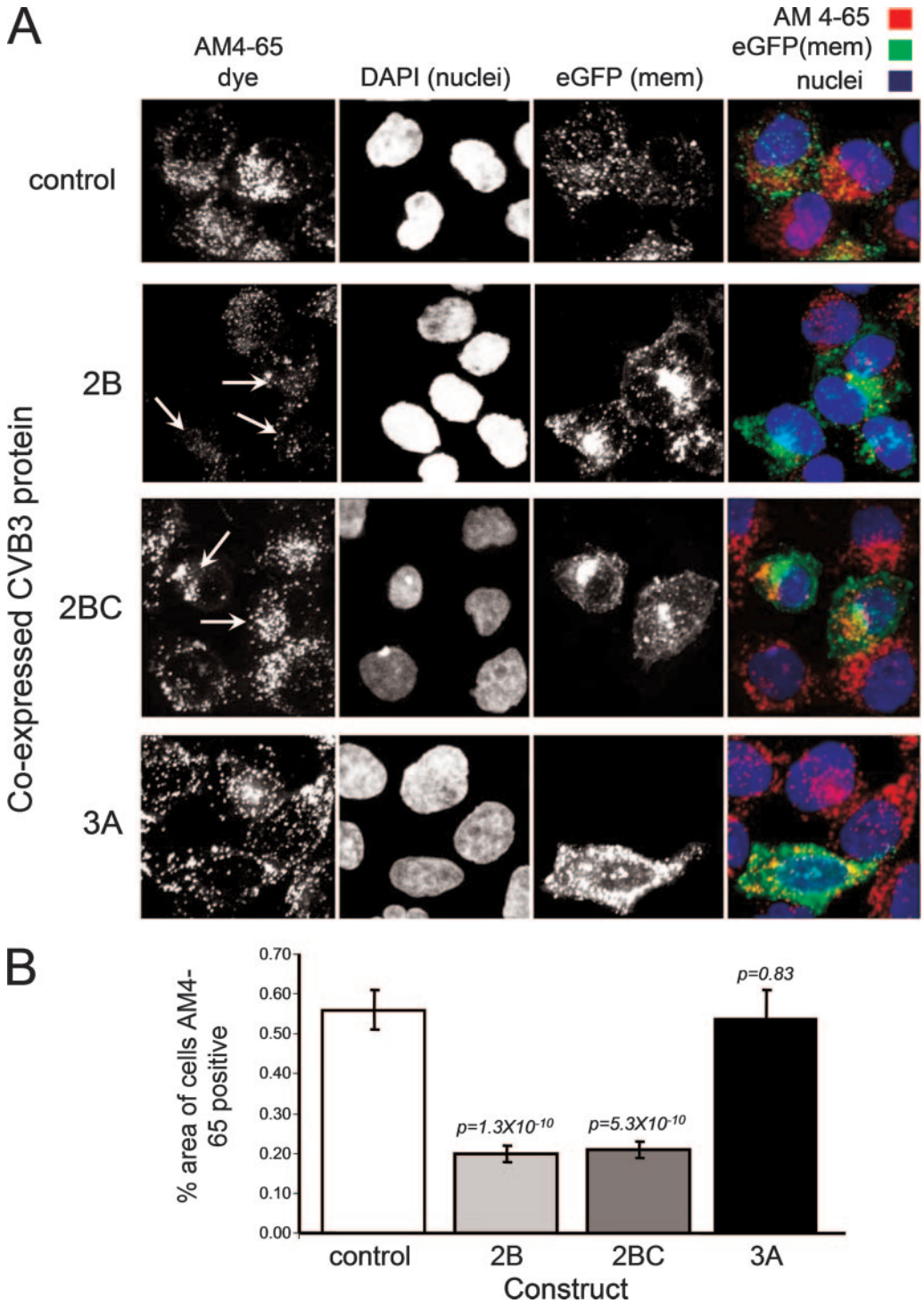

FIG. 7. CVB3 2B and 2BC expression focuses endocytic vesicles to the Golgi compartment. (A) Cells were transfected with each EGFP(mem) dicistronic construct, and at 16 h posttransfection, endosome localization was tracked using the lipophilic styryl dye AM4-65, which fluoresces red (first column) and allows the localization of newly endocytosed vesicles. Nuclei (DAPI staining) and EGFP(mem) signals are depicted in columns two and three, respectively. (B) The ImageJ "analyze particles" feature was utilized to determine the total area of AM4-65 fluorescence in relationship to the total area of the cell across a minimum of 50 cells from three independent experiments. These values were graphed and their standard deviations calculated (error bars). Student's *t* test was done to compare each of the three transfections to the values for the control cell population, and *P* values are given above the bars.

MHC class I trafficking. Initially, we predicted that there would be a logical connection with the antisecretory hierarchy observed in our original study, that is, that the greatest effect on cell surface MHC class I would be seen with the 3A protein (which destroys the Golgi complex), followed by 2BC and 2B (which leave this organelle intact but restrict its throughput). In contrast with these expectations, our results suggest that the downregulation of MHC class I observed during infection represents a synergy between two distinct viral effects which exhibit directional complementarity; 3A shuts off anterograde MHC trafficking by disrupting the Golgi complex, and 2B and/or 2BC induces the rapid internalization of MHC class I molecules that have escaped the net cast by 3A. Increased internalization of MHC class I has been observed in human immunodeficiency virus-infected cells and is attributed to the Nef protein, although the underlying mechanism remains unclear (33), and it has also been reported for cells infected with Kaposi's sarcoma-associated herpesvirus (32). The AM4-65 dye distribution in cells expressing 2B or 2BC and the associated quantitative analysis clearly demonstrated a greatly increased focusing of endosomes around the Golgi complex compared with the case in nontransfected cells. However, the overall number of endosomes varied greatly from cell to cell during these experiments (data not shown), and this, combined with the rapidity of internalization of the dye (measured in seconds), prevented our accurately measuring the rates of endocytosis. We are currently trying to identify the pathway(s) involved in mediating the 2B/2BC internalization effect, which we hypothesize to involve an upregulation of endosome-to-Golgi complex (or *trans*-Golgi complex) transport. Thus far, it has not been determined that any picornavirus proteins participate in direct protein-protein contacts with MHC molecules; whether 2B or 2BC is capable of these interactions is not yet known. However, we propose that the active removal of cell surface components is more likely to be a global effect; none of the data presented herein suggest that the virus-mediated internalization of surface molecules is MHC specific. If this is the case, then other molecules, such as cytokine receptors, may also be downregulated; indeed, this effect has been reported for poliovirus-infected cells and is attributed to the effects of the viral 3A protein (29, 30). Our laboratory is currently evaluating the effects of the 2B and 2BC proteins on other surface molecules, both immunity related and otherwise. Taken together, our data suggest that CVB3 uses two complementary pathways to render the infected cell not only invisible to $CD8^+$ T cells (by removing MHC class I) but also untouchable by several immune effector molecules, such as gamma interferon, tumor necrosis factor, and other critical mediators of the $CD8^+$ T-cell armamentarium.

Our data also show that despite the complete disruption of the Golgi complex, some degree of anterograde MHC class I trafficking occurs in infected cells, as evidenced by the return of nascent MHC even at late times postinfection (Fig. 3C). This result was surprising given the fact that it has been proposed that the vesicular rearrangements induced by CVB3 infection shut off anterograde protein trafficking. Elegant work using poliovirus showed specifically that the presentation of new MHC class I/peptide complexes is inhibited during an infection (9). It is possible that the return of MHC class I to the cell surface despite CVB3 infection represents a cycling of preexisting molecules to and from the surface, from a subcellular compartment that remains functionally intact during CVB3 infection. Nevertheless, at first blush, it is surprising that the viral inhibition of anterograde trafficking is incomplete: what evolutionary advantage might the virus gain through the continued presence of low levels of MHC class I on the surfaces of infected cells? We speculate that by permitting a certain level of MHC expression, CVB3 minimizes detection by natural killer (NK) cells, which are programmed to recognize and kill cells which display extremely low levels of MHC class I (23); perhaps the use of recycled heterodimers (as distinct from heterodimers created de novo within the infected cell and transported to the surface) allows the virus to achieve this effect by using MHC molecules that present innocuous self peptides rather than the viral epitopes that would be more informative to the immune system.

Our findings could provide a possible reason behind the observation that compared to CD8 T cells, antiviral CD4 T cells are much more readily detected during CVB3 infection (35). CD4 T-cell stimulation requires antigen presentation mediated by the MHC class II pathway, which differs from the class I pathway in that it depends on the internalization of exogenous antigens, utilizing the endocytic/lysosomal machinery within the cell. During an infection in vivo, it is possible that this pathway in an infected antigen-presenting cell is left at least partially intact despite the complete virus-mediated disruption of the Golgi complex. In the absence of data which directly assess antigen presentation during CVB3 infection, this possibility cannot be addressed directly. Additionally, picornaviruses have been shown to induce, and utilize for their own benefit, autophagic vesicles in the host cell (22, 24, 38), which can serve to increase MHC class II-dependent antigen presentation (36).

We have also shown in this study that CVB3 RNA replication is necessary for the downregulation of MHC class I molecules (Fig. 3B), which strongly suggests that levels of viral protein(s) generated via the amplification of the input genomic RNA (and subsequent translation of the expanded pool of RNAs) are necessary for this effect. Therefore, in cases where CVB3 virus infection is not productive due to an RNA replication defect, some antigen presentation may still occur in vivo. In the case of virus persistence, it is thought that the viral RNA, in the absence of RNA replication, might exist in a double-stranded form (39). Very low levels of viral protein expression in the absence of RNA amplification could maintain a "smoldering" infection which is unable to be cleared by the host. In turn, this could provoke the immune system-mediated disease associated with CVB3. Importantly, we have shown that the shutoff of host cap-dependent translation is not responsible for the reduction in MHC class I, confirming MHC redistribution rather than a reduction in molar amounts of protein due to translation effects. We also measured the levels of MHC class I by Western blotting using the HLA-ABC antibody employed here and found that none of the CVB3 proteins dramatically affected the overall level of this protein (data not shown).

2B was previously shown to increase membrane permeability in early studies done with poliovirus (2, 27) and has since been classified in the literature as a "viroporin" (1, 31). It has been proposed that 2B self-associates to form pores in cellular mem-

branes (10), which disrupts intracellular calcium homeostasis, thereby increasing membrane permeability and facilitating virus release (43). Interestingly, de Jong and coworkers recently published a study showing that CVB3 2B-mediated calcium efflux from the ER and the Golgi complex mediates inhibition of protein trafficking through these organelles (11). Whether pores actually form inside the infected cell to directly mediate these effects has not yet been shown. While our data regarding the inhibition of trafficking through the Golgi complex are in agreement with the published results, our results point to the possibility that 2B and/or 2BC may additionally upregulate existing trafficking pathways from the plasma membrane to the Golgi complex. This might offer an alternative explanation for published studies that used hygromycin B uptake as a means to measure plasma membrane permeability (2, 10, 27, 44, 45) and could reflect an alteration of certain endocytosis processes (including "bulk-phase" pathways) rather than the formation of nonspecific, perforin-like, membrane-integral pores. This is consistent with the fact that 2B has never been shown to associate directly with the plasma membrane.

The work presented here describes a new picornavirus immune evasion strategy that, in concert with previously identified mechanisms, allows the virus to evade host cell-mediated responses in vivo. Our study also highlights the multifunctional nature of proteins encoded within this small viral genome. Some have argued that picornaviruses have no need to interfere with anterograde trafficking because the rapid shutoff of host protein synthesis should inevitably lead to defective antigen presentation. Our observation that the virus not only diminishes the delivery of cell proteins to the cell surface but also accelerates the removal of existing cellular proteins (perhaps including cytokine receptors) provides an attractive explanation for why these viruses have developed and retained their effects on protein trafficking. Thus, it appears that picornaviruses have evolved to utilize multifunctional proteins that have activities once thought to be reserved for larger viruses, which carry batteries of auxiliary proteins for this purpose.

ACKNOWLEDGMENTS

We thank Annette Lord for excellent secretarial assistance. We also thank Jason Whitmire and Christopher Kemball for technical input regarding flow cytometry.

This work was supported by NIH awards R01 AI-42314 (J.L.W.) and F32 AI-065095 (C.T.C.).

This is manuscript number 18673-MIND from the Scripps Research Institute.

REFERENCES

1. **Agirre, A., A. Barco, L. Carrasco, and J. L. Nieva.** 2002. Viroporin-mediated membrane permeabilization. Pore formation by nonstructural poliovirus 2B protein. J. Biol. Chem. **277:**40434–40441.
2. **Aldabe, R., A. Barco, and L. Carrasco.** 1996. Membrane permeabilization by poliovirus proteins 2B and 2BC. J. Biol. Chem. **271:**23134–23137.
3. **Barco, A., and L. Carrasco.** 1995. A human virus protein, poliovirus protein 2BC, induces membrane proliferation and blocks the exocytic pathway in the yeast Saccharomyces cerevisiae. EMBO J. **14:**3349–3364.
4. **Betz, W. J., F. Mao, and C. B. Smith.** 1996. Imaging exocytosis and endocytosis. Curr. Opin. Neurobiol. **6:**365–371.
5. **Bienz, K., D. Egger, and L. Pasamontes.** 1987. Association of polioviral proteins of the P2 genomic region with the viral replication complex and virus-induced membrane synthesis as visualized by electron microscopic immunocytochemistry and autoradiography. Virology **160:**220–226.
6. **Choe, S. S., D. A. Dodd, and K. Kirkegaard.** 2005. Inhibition of cellular protein secretion by picornaviral 3A proteins. Virology **337:**18–29.
7. **Cornell, C. T., W. B. Kiosses, S. Harkins, and J. L. Whitton.** 2006. Inhibition of protein trafficking by coxsackievirus B3: multiple viral proteins target a single organelle. J. Virol. **80:**6637–6647.
8. **Cornell, C. T., and B. L. Semler.** 2004. Gene expression and replication of picornaviruses, p. 93–117. *In* R. A. Meyers (ed.), Encyclopedia of molecular cell biology and molecular medicine. Wiley-VCH, Weinheim, Germany.
9. **Deitz, S. B., D. A. Dodd, S. Cooper, P. Parham, and K. Kirkegaard.** 2000. MHC I-dependent antigen presentation is inhibited by poliovirus protein 3A. Proc. Natl. Acad. Sci. USA **97:**13790–13795.
10. **de Jong, A. S., W. J. Melchers, D. H. Glaudemans, P. H. Willems, and F. J. Van Kuppeveld.** 2004. Mutational analysis of different regions in the coxsackievirus 2B protein: requirements for homo-multimerization, membrane permeabilization, subcellular localization, and virus replication. J. Biol. Chem. **279:**19924–19935.
11. **de Jong, A. S., H. J. Visch, F. de Mattia, M. M. van Dommelen, H. G. Swarts, T. Luyten, G. Callewaert, W. J. Melchers, P. H. Willems, and F. J. Van Kuppeveld.** 2006. The coxsackievirus 2B protein increases efflux of ions from the endoplasmic reticulum and Golgi, thereby inhibiting protein trafficking through the Golgi. J. Biol. Chem. **281:**14144–14150.
12. **de Jong, A. S., E. Wessels, H. B. Dijkman, J. M. Galama, W. J. Melchers, P. H. Willems, and F. J. Van Kuppeveld.** 2003. Determinants for membrane association and permeabilization of the coxsackievirus 2B protein and the identification of the Golgi complex as the target organelle. J. Biol. Chem. **278:**1012–1021.
13. **Dodd, D. A., T. H. Giddings, Jr., and K. Kirkegaard.** 2001. Poliovirus 3A protein limits interleukin-6 (IL-6), IL-8, and beta interferon secretion during viral infection. J. Virol. **75:**8158–8165.
14. **Doedens, J. R., T. H. Giddings, and K. Kirkegaard.** 1997. Inhibition of endoplasmic reticulum-to-Golgi traffic by poliovirus protein 3A: genetic and ultrastructural analysis. J. Virol. **71:**9054–9064.
15. **Doedens, J. R., and K. Kirkegaard.** 1995. Inhibition of cellular protein secretion by poliovirus proteins 2B and 3A. EMBO J. **14:**894–907.
16. **Donaldson, J. G., D. Finazzi, and R. D. Klausner.** 1992. Brefeldin A inhibits Golgi membrane-catalysed exchange of guanine nucleotide onto ARF protein. Nature **360:**350–352.
17. **Echeverri, A. C., and A. Dasgupta.** 1995. Amino terminal regions of poliovirus 2C protein mediate membrane binding. Virology **208:**540–553.
18. **Egger, D., R. Gosert, and K. Bienz.** 2002. Role of cellular structures in viral RNA replication, p. 247–253. *In* B. L. Semler and E. Wimmer (ed.), Molecular biology of picornaviruses. ASM Press, Washington, DC.
19. **Eggers, H. J.** 1982. Benzimidazoles. Selective inhibitors of picornavirus replication in cell culture and in the organism, p. 377–417. *In* P. E. Came and L. A. Caliguiri (ed.), Chemotherapy of viral infections. Springer-Verlag, New York, NY.
20. **Feuer, R., I. Mena, R. Pagarigan, M. K. Slifka, and J. L. Whitton.** 2002. Cell cycle status affects coxsackievirus replication, persistence, and reactivation in vitro. J. Virol. **76:**4430–4440.
21. **Finlay, B. B., and G. McFadden.** 2006. Anti-immunology: evasion of the host immune system by bacterial and viral pathogens. Cell **124:**767–782.
22. **Jackson, W. T., T. H. Giddings, Jr., M. P. Taylor, S. Mulinyawe, M. Rabinovitch, R. R. Kopito, and K. Kirkegaard.** 2005. Subversion of cellular autophagosomal machinery by RNA viruses. PLoS Biol. **3:**e156.
23. **Karre, K., H. G. Ljunggren, G. Piontek, and R. Kiessling.** 1986. Selective rejection of H-2-deficient lymphoma variants suggests alternative immune defence strategy. Nature **319:**675–678.
24. **Kirkegaard, K., M. P. Taylor, and W. T. Jackson.** 2004. Cellular autophagy: surrender, avoidance and subversion by microorganisms. Nat. Rev. Microbiol. **2:**301–314.
25. **Knowlton, K. U., E. S. Jeon, N. Berkley, R. Wessely, and S. Huber.** 1996. A mutation in the puff region of VP2 attenuates the myocarditic phenotype of an infectious cDNA of the Woodruff variant of coxsackievirus B3. J. Virol. **70:**7811–7818.
26. **Kuechler, E., J. Seipelt, H. D. Liebig, and W. Sommergruber.** 2002. Picornavirus proteinase-mediated shutoff of host cell translation: direct cleavage of a cellular initiation factor, p. 301–312. *In* B. L. Semler and E. Wimmer (ed.), Molecular biology of picornaviruses. ASM Press, Washington, DC.
27. **Lama, J., and L. Carrasco.** 1992. Expression of poliovirus nonstructural proteins in Escherichia coli cells. Modification of membrane permeability induced by 2B and 3A. J. Biol. Chem. **267:**15932–15937.
28. **Moffat, K., G. Howell, C. Knox, G. J. Belsham, P. Monaghan, M. D. Ryan, and T. Wileman.** 2005. Effects of foot-and-mouth disease virus nonstructural proteins on the structure and function of the early secretory pathway: 2BC but not 3A blocks endoplasmic reticulum-to-Golgi transport. J. Virol. **79:**4382–4395.
29. **Neznanov, N., K. P. Chumakov, A. Ullrich, V. I. Agol, and A. V. Gudkov.** 2002. Unstable receptors disappear from cell surface during poliovirus infection. Med. Sci. Monit. **8:**BR391–BR396.
30. **Neznanov, N., A. Kondratova, K. M. Chumakov, B. Angres, B. Zhumabayeva, V. I. Agol, and A. V. Gudkov.** 2001. Poliovirus protein 3A inhibits tumor necrosis factor (TNF)-induced apoptosis by eliminating the TNF receptor from the cell surface. J. Virol. **75:**10409–10420.
31. **Nieva, J. L., A. Agirre, S. Nir, and L. Carrasco.** 2003. Mechanisms of

membrane permeabilization by picornavirus 2B viroporin. FEBS Lett. **552:** 68–73.
32. **Paulson, E., C. Tran, K. Collins, and K. Fruh.** 2001. KSHV-K5 inhibits phosphorylation of the major histocompatibility complex class I cytoplasmic tail. Virology **288:**369–378.
33. **Piguet, V., L. Wan, C. Borel, A. Mangasarian, N. Demaurex, G. Thomas, and D. Trono.** 2000. HIV-1 Nef protein binds to the cellular protein PACS-1 to downregulate class I major histocompatibility complexes. Nat. Cell Biol. **2:**163–167.
34. **Sanz-Parra, A., F. Sobrino, and V. Ley.** 1998. Infection with foot-and-mouth disease virus results in a rapid reduction of MHC class I surface expression. J. Gen. Virol. **79:**433–436.
35. **Slifka, M. K., R. Pagarigan, I. Mena, R. Feuer, and J. L. Whitton.** 2001. Using recombinant coxsackievirus B3 to evaluate the induction and protective efficacy of $CD8^+$ T cells during picornavirus infection. J. Virol. **75:**2377–2387.
36. **Strawbridge, A. B., and J. S. Blum.** 2007. Autophagy in MHC class II antigen processing. Curr. Opin. Immunol. **19:**87–92.
37. **Sugawara, S., T. Abo, and K. Kumagai.** 1987. A simple method to eliminate the antigenicity of surface class I MHC molecules from the membrane of viable cells by acid treatment at pH 3. J. Immunol. Methods **100:**83–90.
38. **Suhy, D. A., T. H. Giddings, Jr., and K. Kirkegaard.** 2000. Remodeling the endoplasmic reticulum by poliovirus infection and by individual viral proteins: an autophagy-like origin for virus-induced vesicles. J. Virol. **74:**8953–8965.
39. **Tam, P. E., and R. P. Messner.** 1999. Molecular mechanisms of coxsackievirus persistence in chronic inflammatory myopathy: viral RNA persists through formation of a double-stranded complex without associated genomic mutations or evolution. J. Virol. **73:**10113–10121.
40. **Tershak, D. R.** 1984. Association of poliovirus proteins with the endoplasmic reticulum. J. Virol. **52:**777–783.
41. **Teterina, N. L., A. E. Gorbalenya, D. Egger, K. Bienz, and E. Ehrenfeld.** 1997. Poliovirus 2C protein determinants of membrane binding and rearrangements in mammalian cells. J. Virol. **71:**8962–8972.
42. **Van Kuppeveld, F. J., A. S. de Jong, W. J. Melchers, and P. H. Willems.** 2005. Enterovirus protein 2B po(u)res out the calcium: a viral strategy to survive? Trends Microbiol. **13:**41–44.
43. **Van Kuppeveld, F. J., J. G. Hoenderop, R. L. Smeets, P. H. Willems, H. B. Dijkman, J. M. Galama, and W. J. Melchers.** 1997. Coxsackievirus protein 2B modifies endoplasmic reticulum membrane and plasma membrane permeability and facilitates virus release. EMBO J. **16:**3519–3532.
44. **Van Kuppeveld, F. J., W. J. Melchers, K. Kirkegaard, and J. R. Doedens.** 1997. Structure-function analysis of coxsackie B3 virus protein 2B. Virology **227:**111–118.
45. **Van Kuppeveld, F. J., P. J. van den Hurk, J. Zoll, J. M. Galama, and W. J. Melchers.** 1996. Mutagenesis of the coxsackie B3 virus 2B/2C cleavage site: determinants of processing efficiency and effects on viral replication. J. Virol. **70:**7632–7640.
46. **Whitton, J. L., and M. B. A. Oldstone.** 2001. The immune responses to viruses, p. 285–320. *In* D. M. Knipe, P. M. Howley, D. E. Griffin, R. A. Lamb, M. A. Martin, B. Roizman, and S. E. Straus (ed.), Fields virology. Lippincott Williams & Wilkins, Philadelphia, PA.